Sensors and Materials, Vol. 36, No. 8 (2024) 3335–3350
MYU Tokyo

S & M 3735

Remote Charging for Cardiac Pacemakers Using Transcutaneous Optical Energy Transmission System

Shang-Kuo Yang,[1] Chia-Hong Chen,[1] Yong-Jun Zhu,[2] and Kai-Jung Chen[1*]

[1]Department of Mechanical Engineering, National Chin Yi University of Technology, Taichung 41170, Taiwan, R.O.C.
[2]School of Electronic and Information Engineering, Suzhou University of Science and Technology, Suzhou 215009, Jiangsu, P.R.C.

(Received March 11, 2024; accepted April 30, 2024)

Keywords: transcutaneous optical energy transmission system, pacemaker, remote charging

For cardiopathy patients with an implanted cardiac pacemaker, supplying power to the pacemaker is a challenging problem. In this study, we aim to design a transcutaneous optical energy transmission system that transmits optical energy from an optical-energy-generating circuit to a receiving circuit in a human body through the skin to charge the pacemaker's battery such that the battery supplies power to the pacemaker continuously. We use 0.5-mm-thick pigskin to imitate human skin tissue. The light source of the system is a halogen lamp and the receiver is a solar cell. The beam emitted by a the halogen lamp is transmitted to the solar cell through the skin generating a photovoltaic effect so as to charge the rechargeable button battery. As optical energy is received by a four-solar-cell module, we adopt a Zener voltage regulation circuit and a pure resistance circuit to charge the battery. Experimental data show that if a four-solar-cell module is used to charge a battery with the voltage regulation circuit, the battery after 62 h of charging stores enough power to operate the pacemaker for 20–35 days. On the other hand, charging the battery using the pure resistor circuit can reduce the charging time from 62 h to 14 h for the same number of operation days. If the number of solar cells in parallel is increased to 12, the charging time for the same number of operation days can be shortened from 14 h to 12 h with the pure resistance circuit. As a result, transcutaneous remote charging is achieved. Approaches to shorten the charging time and future works are proposed as well.

1. Introduction

1.1 Research motivation

For patients with implanted cardiac pacemakers, the power supply for the pacemaker poses a challenging issue. The motivation of this study is to solve the charging problem for patients with implanted pacemakers. In early prototypes, pacemakers were powered by large power suppliers,[(1)] which imposed restrictions on patients' mobility. With advancements in battery technology and the introduction of coin batteries, pacemakers can now be powered by a single

*Corresponding author: e-mail: hskchen5@ncut.edu.tw
https://doi.org/10.18494/SAM5039

ISSN 0914-4935
https://myukk.org/

coin battery, eliminating the inconvenience of using bulky power supply equipment in the previous generation of devices. This improvement simplifies the power supply and enhances the patients' mobility. However, because of the limited capacity of the coin battery, the pacemaker cannot work once the battery is depleted. In other words, if a patient with an implanted pacemaker has a long lifespan, this person will require surgical procedures to replace the pacemaker's battery or upgrade the entire pacemaker once the battery is drained. This increases the medical costs and introduces associated risks and discomfort during surgery for the patients. The application of rechargeable coin batteries for powering pacemakers has led to the development of transcutaneous remote charging technology. A review of the past literature on transcutaneous remote charging reveals that coil-based energy transmission media were predominantly used. The system employed a primary coil as the external energy generation device and a secondary coil as the internal energy receiving device.(2,3) In the current study, a transcutaneous optical energy transmission (TOET) system is proposed, where a halogen lamp is utilized as the transcutaneous optical energy generation medium and a solar cell as the transcutaneous optical-energy-receiving medium. This system transfers optical energy to charge a rechargeable coin battery inside the body, which deviates from the employment of coil-based energy generation and reception media in transcutaneous energy transmission (TET) systems reported in previous literature.

1.2 Literature review

The use of rechargeable coin batteries in heart rhythm regulators gave rise to transcutaneous remote charging technology. Looking back at the past literature of percutaneous remote charging, it can be seen that coils were used as percutaneous energy transmission media, that is, the primary coil was used as an energy generation device and the secondary coil was *in vitro*. This architecture has been extensively studied in the past, such as in the electrohydraulic total artificial heart system (EHTAH)(2) and implantable artificial myocardium system.(3) Nowadays, many forms of remote charging exist, for example, the remote energy transmission mode of pulsed light(4) and the remote energy transmission mode of a DC-to-DC converter.(5) For both the above two forms, the primary and secondary coils (or winding) are the energy transmission media used.(5)

The methods described above can achieve TET; however, the use of coil energy transmission still has disadvantages. One is the shielding effect,(6) which is a problem of interference in an electromagnetic environment. If an aluminum can is placed close to the primary and secondary windings, as the distance between them decreases, the coil's equivalent resistance will increase. However, if the primary and secondary coils were covered by an amorphous silicon layer, the shielding effect of the coil decreased, resulting in a significant reduction in equivalent series resistance. However, some equivalent series resistance still remains. An energy transmission system called a transcutaneous transformer was applied in an experiment.(7) According to its experimental data, with a transmission power of 24 W and a coil separation distance of 0.5 cm, the power losses resulting from the transdermal transformer, the rectifier circuit, and the control circuit are about 4, 12, and 6% of the total power, respectively. In other words, there is a power loss of about 22% when transcutaneous energy is received, among which the transformer (with coil parts) accounts for nearly 20%.[7] Consequently, the coil structure and the shielding effect for transdermal energy transmission lose significant power. Therefore, other energy media must be investigated for transdermal energy transmission.

2. Transcutaneous Optical Energy Transmission System

The energy transmission, generation, and receiving media of the TOET system used in this study differ from those of a traditional TET system. The concept of this study is derived from the transcutaneous optical telemetry (TOT) system.[8] To establish a TOET system, the energy-generating and energy-receiving media used in a TET system should be replaced by a laser diode (LD)/halogen lamp[9] and a solar cell, respectively, as shown in Fig 1. The TOET system established in this study has the merit of avoiding the shielding effect and power loss caused by using coils in a TET system.

2.1 Energy-generating and energy-receiving media

As shown in Fig. 2, the relative spectral response sensitivity peaks of silicon (Si) and amorphous Si solar cells are about 0.8–1.0 and 0.6 µm, respectively.[9] Therefore, the wavelength of the optical-energy-generating medium should be 0.8–1.0 or 0.6 µm so as to make the photoelectric conversion of a solar cell efficient. Experiments were successfully carried out using silicon solar cells as the light-energy-receiving media.[9] There are two issues that affect the photoelectric conversion of solar cells: the wavelength of the light beam focused on the solar cell and the electric power of the beam. The material of the solar cell determines the wavelength of the execution light; then, the photoelectric conversion of the solar cell can be determined merely by adjusting the optical power of the light beam. If a halogen lamp is chosen as the light source, the light penetration and reflectivity agree with conditions of a LD. Since the induction sensitivity of the solar cell is based on the wavelength of the optical-energy-generating medium,

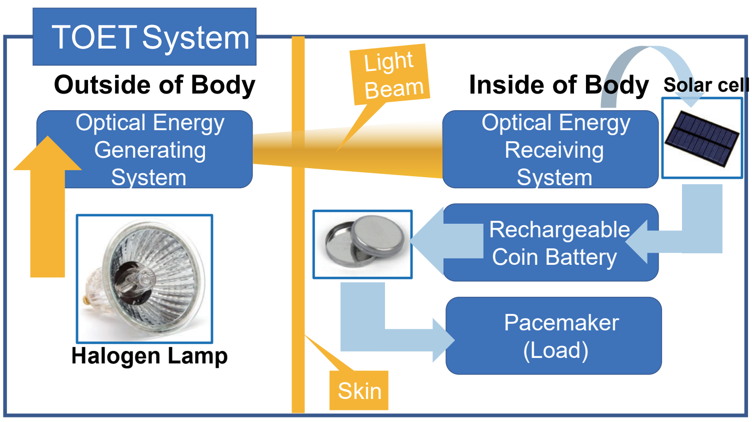

Fig. 1. (Color online) Concept of the TOET system.

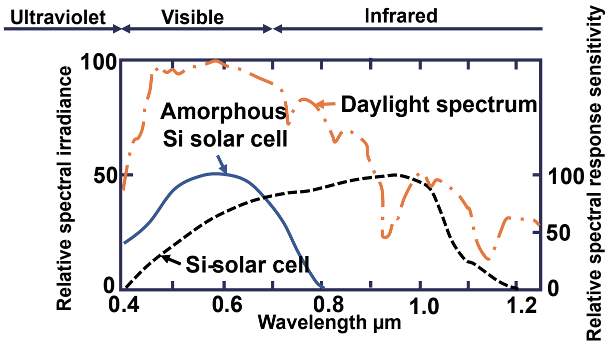

Fig. 2. (Color online) Spectrum of relative spectral response sensitivity for solar cells.(9)

a halogen lamp that emits a 0.6 μm wavelength is the best choice for an amorphous silicon solar cell. In this study, we adopt a Halotone GU 5.3 halogen lamp made by Philips Company to transmit optical energy. Relevant specifications of the lamp are as follows: electric power consumption of 50 W, ultraviolet light wavelength range from 185 to 380 nm, visible light wavelength range from 380 to 780 nm, and near-infrared light wavelength range from 780 to 3000 nm, as shown in Fig. 3.(10) For this study, SC-2723 solar cells of the SC series from SINONAR CORP(11) are chosen as the media for receiving light energy. These solar cells can convert light waves with a wavelength of approximate 0.6 μm. Furthermore, if paired with another halogen lamp with a wavelength of about 0.81 μm, three/five groups or silicon solar cells can be cooperated to use.

2.2 Optical-energy-receiving circuit

The functions of the components in the optical-energy-receiving circuit shown in Fig. 4 are described as follows.

1. The solar cell senses the light of a specific light spectrum to induce photoelectric conversion via the photovoltaic effect.
2. R1 is the series resistance of the Zener diode and determines the Zener current.
3. The model number of the Zener diode is RD3.0UH.(12) The relevant specifications are as follows: Zener voltage of 3.0 V (average), internal resistance of 360 Ω, Zener test current I_{ZT} = 0.5 mA, Zener knee current I_{ZK} = 0.05 mA, and Zener maximum current I_{ZM} = 1.2 mA.
4. By setting suitable values of input voltage and R1, the desired regulated voltage (V_Z) can be obtained.
5. Schottky diode D1 has a higher switching response than do ordinary rectifier diodes. D1 is used to prevent current backflow from the coin battery to the solar cell and is also known as a countercurrent protection diode.
6. R2 is a low-resistance resistor that is used to determine the circuit current from its voltage drop.
7. The rechargeable coin battery is a single chargeable button battery (model no. ML2430; Sanyo Company). Its bottom voltage is 2.0 V, the full load voltage is 3.0 V, and the power storage is 100 mAh, as shown in Fig. 5.(13)

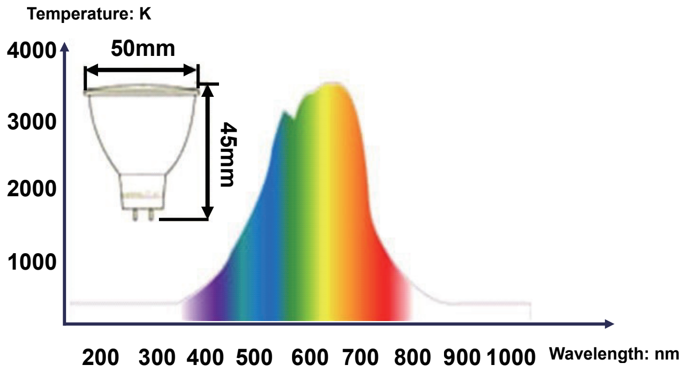

Fig. 3. (Color online) Spectrum of Halotone GU 5.3 halogen lamp.[10]

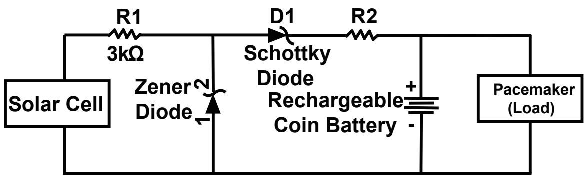

Fig. 4. Voltage regulation circuit of the light-energy-receiving circuit.

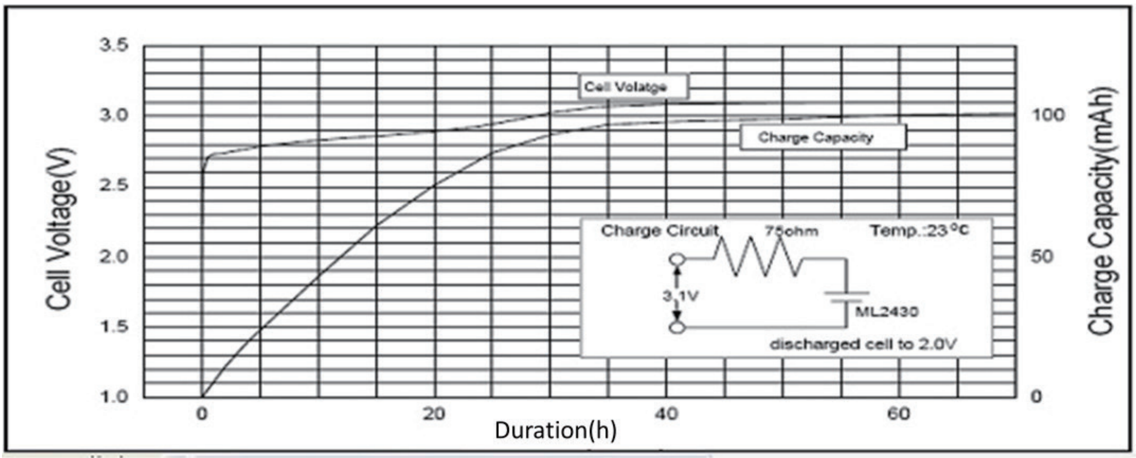

Fig. 5. Charge characteristics of ML2430 battery.[13]

8. The load is a cardiac pacemaker. There are many types of pacemaker. According to the NASPE Association's pacemaker coding table,[14] a DDDR type of rhythm regulator is a dual-chamber pacing, dual-chamber sensing, dual-chamber response to sensing, and rate-responsive regulator. The object of this study is a DDDR type, which requires an open circuit voltage of 2.8 V and an average short-circuit current of 21 μA in total demand.[15] The frequency response of the pacemaker is adjusted by changing the output frequency of the internal circuit in accordance with the patient's heart rhythm needs.

2.3 Thermal effect of optical energy on biological tissue

To discuss the effect of temperature on biological tissue, we must first define the safe temperature of the thermal effect on biological tissue; biological tissue here refers to the epidermal tissue of human skin.(14) Thermal activation occurs when the temperature of the human epidermis is between 36.5 and 40 °C. Above 40 °C, the protein denaturation reaction begins; the coagulation reaction begins at 68 °C; and the vaporization reaction begins above 100 °C. Above 500 °C, the carbonization reaction occurs. In summary, an ambient temperature below 40 °C is safe for human skin.

In this study, we use 0.5-mm-thick pigskin to imitate human skin tissue. The steps to determine the minimum safe distance between the halogen lamp and the pigskin are as follows. Starting with a distance of 20 cm, we keep this distance for 3 to 4 min, then measure and record the skin temperature. Afterward, we decrease the distance by 1 cm at a time and repeat this step until the distance is 1 cm. The experimental setup is shown in Fig. 6. Figure 7 shows the experimental data. Since temperatures below 40 °C present no danger to human skin, it is seen

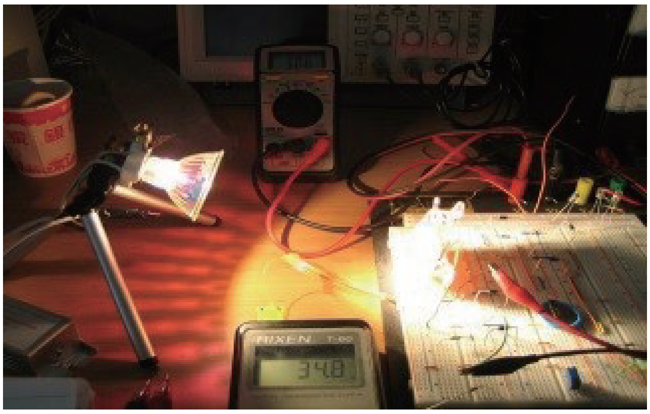

Fig. 6. (Color online) Experimental setup of the system.

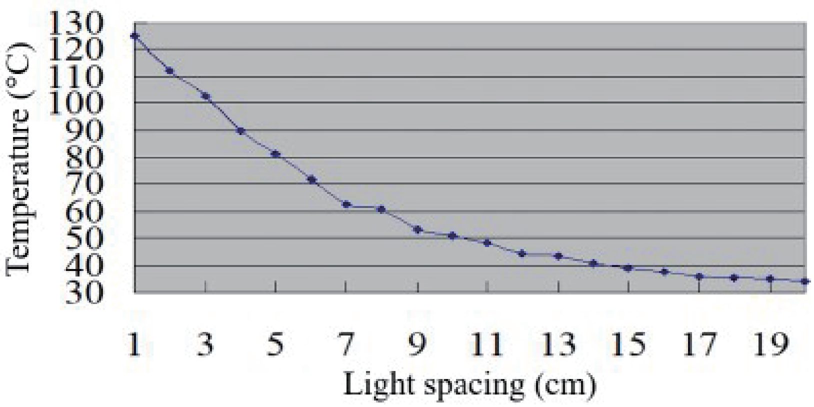

Fig. 7. (Color online) Plot of light spacing versus temperature of pigskin.

that the distance of 16 cm is a good choice. Once the safe distance was defined as 16 cm, the 24-h long-term effect should be validated. The skin temperature versus continuous irradiation time at the distance of 16 cm is shown in Fig. 8. The temperature of the skin remains at about 37 °C, which falls below the threshold temperature of 40 °C.

3. Experiments for the TOET System

3.1 Coin battery voltage measurement

In the current study, the voltage of a rechargeable battery is defined as constant voltage. Constant voltage means that the battery voltage remains at an approximately fixed value for a considerably long time. To charge a rechargeable battery, the process should begin from the bottom voltage of 2.0 V for the ML2430 battery. The voltage curve of the ML2430 battery during charging is shown in Fig. 9. The voltage of the battery that has just been continuously charged for 12 h is called the initial voltage but it is not a constant voltage. The stage at which the

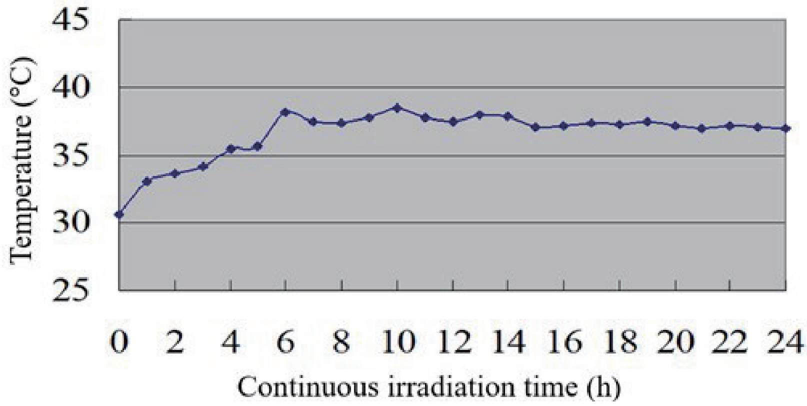

Fig. 8. (Color online) Skin temperature versus continuous irradiation time at the distance of 16 cm.

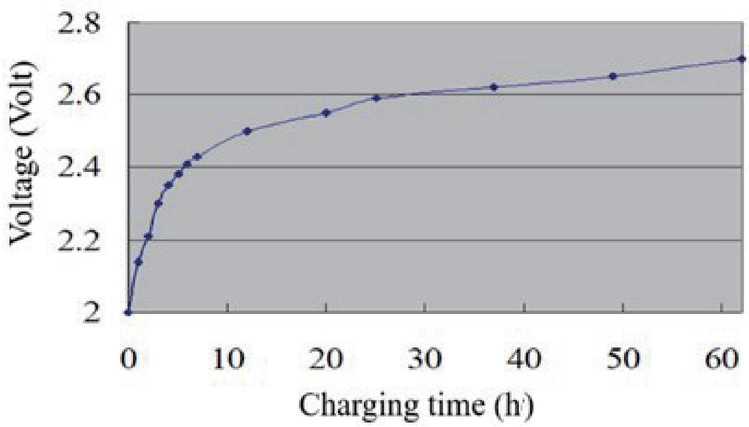

Fig. 9. (Color online) Voltage curve of the ML2430 battery during charging.

voltage returns from the initial voltage to the constant voltage is known as the returning stage. The returning stage is part of the battery static process; during this time, the battery voltage returns to the constant voltage. The just-charged battery must be held static for about 6 h to cross into the returning stage, after which the measured battery voltage is the constant voltage, as shown in Fig. 10.

The next recharging process should also begin from the bottom voltage, so the charged battery must be discharged for about 3 to 4 h until the bottom voltage is reached. However, if the battery voltage drops below the lower threshold voltage after discharging, it needs to be charged back up to the lower threshold voltage.

As shown in Fig. 9, the charging curve of a coin-type battery has two phases: the rapid rising phase followed by the slow rising phase. The voltage of the rechargeable battery obtained by the regulator circuit of the TOET system after 62 h of charging is 2.73 V, and this voltage corresponds to an ampere-hour value of 10 mAh.[13]

3.2 Power measurement

To measure the power received by the solar cells, we use the optical power measuring instrument NOVA II of OPHIR Company. Figure 11 shows the received electric powers (mW) when the optical power sensor was (a) uncovered and (b) covered by pigskin versus spacing between the optical power sensor and the halogen lamp (optical wavelength of 633 nm). At the safe distance of 16 cm and with the pigskin optical transmittance of 13.5%, read from Fig. 11(b), the covered optical power is 6.8 mW. This optical power can provide enough energy for the solar cell to charge the rechargeable button battery.

The rated charging voltage for the rechargeable button-type battery in this study is 2.8–3.25 V.[13] Unfortunately, a single solar cell of the optical energy harvesting circuit under illumination

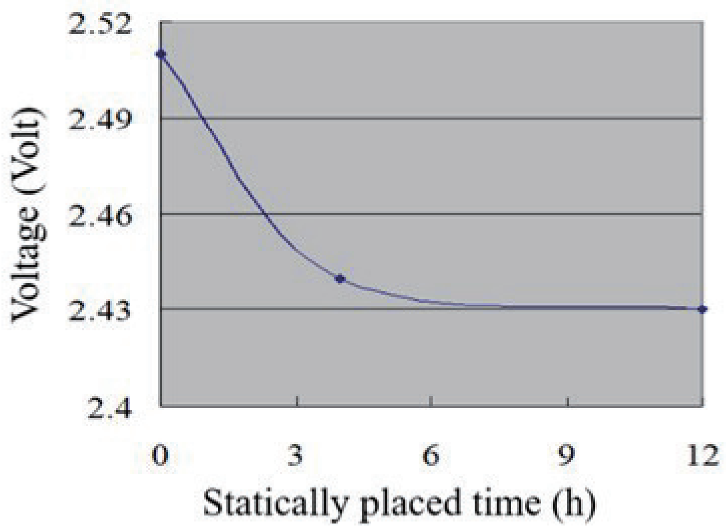

Fig. 10. (Color online) Returning stage of a coin-type rechargeable battery.

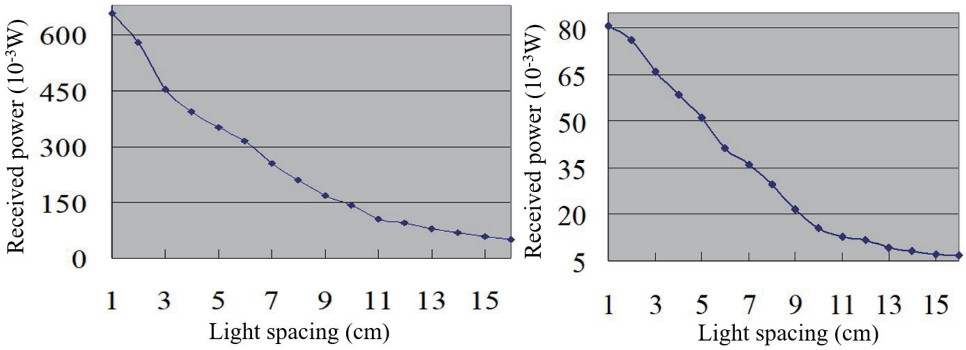

Fig. 11. (Color online) Received power (mW) versus spacing: (a) uncovered and (b) covered.

cannot acquire this rated charging voltage. Four solar cells in parallel are employed to solve this problem. Figure 12 shows the voltage regulator outputs of the optical energy receiving circuit versus different light spacings for one and four solar cells. It is evident from Fig. 12 that the light spacing should be less than 13 cm in order to obtain the rated charging voltage by using a single solar cell. Unfortunately, this conflicts with the 16 cm safe illumination distance. Using four solar cells in parallel can meet the requirement.

3.3 Problem of pigskin moisturizing

According to the results of experiments, fresh pigskin tends to lose moisture over time. The moisture of fresh pigskin decreased after approximately 5 to 6 h, as shown in Fig. 13. To maintain the freshness of the pigskin, it is necessary to replace it at least every 4 h. The light transmittance of the pigskin gradually increases owing to the gradual loss of moisture. The light transmittances of fresh pigskin under continuous illumination are 11–14% for 0–4 h, 16–18% for 5–7 h, and 22–35% for 8–12 h. The relationship between the optical transmittance of the pigskin and irradiation time is shown in Fig. 14. The more rapid the loss of the moisture of the pigskin, the faster the increase in light transmittance.

3.4 Endurance of charged battery

The number of sustainable working days, L, of the charged battery for operating the pacemaker in this study can be calculated as

$$L = \frac{Q}{24 \times I}, \tag{1}$$

where Q is the number of ampere-hours of the battery and I is the consumption current amperage of the pacemaker. Using the current consumption data (Table 1),[15] L is calculated to be 35 days in the sensing mode and 20 days in the full load.

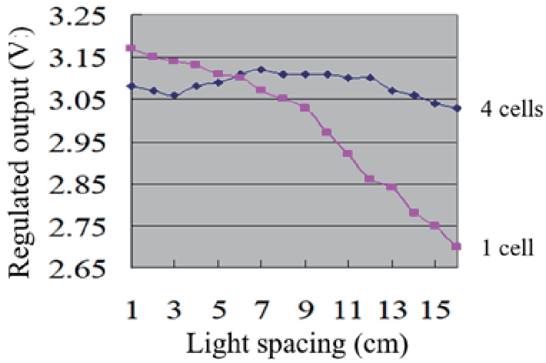

Fig. 12. (Color online) Regulated output voltages of one solar cell and four solar cells in parallel versus spacing.

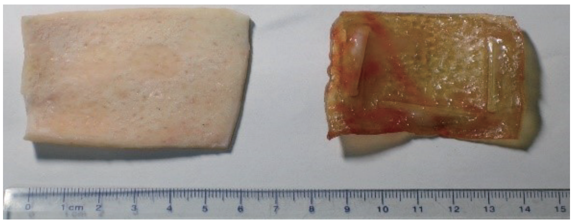

Fig. 13. (Color online) Fresh and moisture-drained pigskin samples.

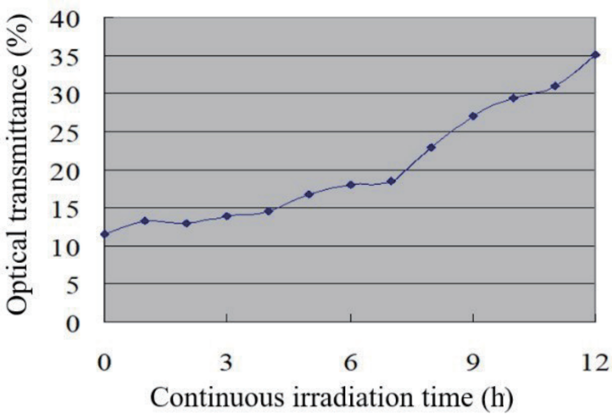

Fig. 14. (Color online) Optical transmittance of the pigskin versus irradiation time.

Table 1
Average current consumption for functions of a pacemaker.[15]

Function	Peak current drain	Average current drain	Average current drain as percentage of total (%)
Pacing current	7 mA	8 μA	38
Sense amplifier	2 μA	2 μA	10
Rate adaptive sensor	2 μA	2 μA	10
Control	16 μA	8 μA	38
Telemetry	60 μA	<1 μA	4
Total	N/A	21 μA	100

4. Discussion

4.1 Time needed for charging the battery

The findings described in Sect. 3.1 reveal that the battery requires a continuous charge of 62 h to attain 2.73 V and 10 mAh, which falls short of the actual requirements. The long charging time results from the insufficient charging current of the Zener voltage regulator circuit used in the charging circuit, while the insufficient current is caused by the excessive resistance of the Zener series resistor R1. The R1 value used in this study is indeed greater than that recommended in the ML battery series specification.(13) Therefore, reducing the R1 value can increase the charging current. However, if the solar cells do not provide enough electric power, the solar cells may not provide sufficient current to charge the battery.

Unlike the DC power supply, the solar cell power situation is not ideal. In comparing the above two types of power supply, results from an experiment showed that the no-load voltage of both was 3.68 V, whereas the loaded output voltage of the solar cell dropped to 2.76 V, while the output voltage of the DC power supply remained at 3.68 V with the same load. This phenomenon is the so-called load effect of a voltage source. In this study, the power provided by the solar cell after charging was 5.21 mW. In contrast, the power provided by the DC power supply was 38.56 mW. The difference between the two is 7.4 times, so the charging time of the solar cell is longer.

4.2 Approaches to shorten charging time

4.2.1 Using two-stage charging regulator circuit

The current required by the battery during the period of rapidly rising voltage is large. During this period, V_Z can be relaxed to a higher value. This will allow the battery to pass through the period of rapidly rising voltage more quickly. Conversely, in the slow voltage-rising period, the battery requires minimal current. At this stage, reverting to the original Zener diode value is advisable to prevent excessive charging current from damaging the battery. Thus, the Zener diode should be switched back to the original one at this stage to avoid damage to the battery caused by excessive charging current. The experiment shows that the battery voltage increased quickly and then slowly after reaching 2.50 V in the charging process. After 12 h of charging by the two-stage voltage regulator circuit, the constant voltage of the battery is 2.59 V, whereas it is 2.50 V when using the original Zener circuit. Therefore, two-stage voltage regulator charging can shorten the duration of the period of rapidly rising voltage.

Figure 15 shows the two-stage charging circuit. During the first stage, the V_Z = 4.5 V Zener diode is used to charge the battery by setting Switch 1 to OPEN and Switch 2 to CLOSE. After approximately 8 h, the constant voltage of the battery reaches 2.50 V, then the original Zener diode with V_Z = 3.0 V is used to charge the battery by setting Switch 1 to CLOSE and Switch 2 to OPEN.

The constant voltage of the battery after 12 h of charging by the two-stage charging voltage regulator circuit is 2.59 V, whereas it is 2.50 V when using the single charging voltage regulator

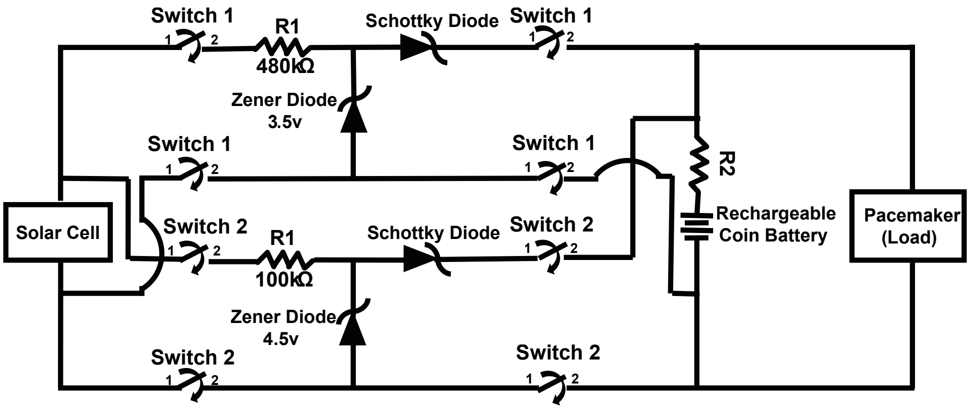

Fig. 15. Two-stage voltage regulator circuit.

circuit. Therefore, under the same charging time, the amount of increase in the battery voltage of the two-stage charging regulator circuit is larger than that of the single charging regulator circuit.

4.2.2 Using pure resistance charging circuit

Another method to reduce the charging time is to use a pure resistance charging circuit, as shown in Fig. 16, instead of the original Zener voltage regulator circuit. According to experimental results, the output power of the Zener circuit connected with four solar cells is 5.21 mW, while it is 8.03 mW for the pure resistance circuit. The results are listed in Table 2. The reason for the increased power is the use of a low-resistance resistor (68 Ω) in the pure resistance circuit, the resistance of which is much lower than that (3 kΩ) in the Zener regulated voltage circuit. This results in the increase in charging current from 1.30 to 2.91 mA. It takes only 14 h to charge the battery to 2.66 V using the pure resistance circuit. Accordingly, increasing the charging current can effectively reduce the battery charging time.

4.2.3 Increasing the electric power of solar cells

Without doubt, the electric power most affects the battery charging time. Since the electric power of the existing solar cells is limited, disregarding the occupied space, in this study, we increase the number of existing solar cell modules (comprising four solar cells in parallel) from 1 to 3. The more modules are used, the more the charging current and electric power of the circuit increase. The output voltage, however, remains relatively stable. The results obtained from the conducted experiment show that one module generates 8.03 mW and three modules produce 16.24 mW, as shown in Fig. 17. The required charging times of the pure resistance circuit with one module are 14 h to achieve a battery voltage of 2.66 V, while using three modules achieves a voltage of 2.73 V in just 12 h.

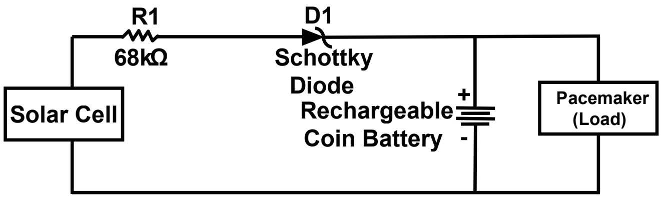

Fig. 16. (Color online) Pure resistance charging circuit.

Table 2
Experimental data of Zener regulation and pure resistance circuits with four parallel solar cells.

	Zener regulation circuit	Pure resistance circuit
Output voltage (V)	3.43	2.76
Output current (mA)	1.52	2.91
Charging current (mA)	1.30	2.91
Output power (mW)	5.21	8.03
Charging time (h)	62	14
Battery voltage after charging (V)	2.73	2.66

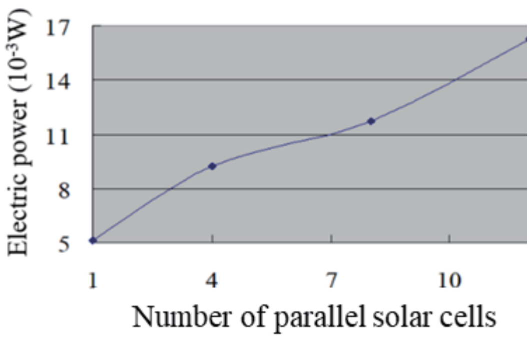

Fig. 17. (Color online) Electric powers generated with various numbers of parallel solar cells.

5. Future Works

Regarding the efforts described above, the charging time of 12 h and the endurance of 20 to 35 days for the pacemaker are still insufficient for practical application. With respect to the scheme proposed in this study, three potential issues should be further considered in the future.

1. For optimal compatibility with a pacemaker, the solar cell size must be small enough to fit the pacemaker's actual size. In addition, the power generated by the solar cell should be closer to the ideal power supply so that the output voltage and current of the supply circuit can be sufficient without the occurrence of the load effect and the battery charging time can be effectively shortened. Therefore, a smaller solar cell module with a higher electric power is expected.
2. To improve the light source used for charging, an optical source with higher light power and light beam concentration without causing damage to the skin should be employed instead of

the halogen lamp used in this study. The concentration of the beam used in this study is insufficient at distances greater than the safe spacing. The light power emitted by the Philips halogen lamp at the safe spacing is about 53 mW, but the optical power received by the transdermal solar cell is only 6.8 mW. The solar cell's performance hinges on its ability to absorb sufficient optical power for efficient photoelectric conversion. Consequently, the chosen light source ought to possess higher optical power and superior beam concentration. However, it is essential to consider the potential heating effect on the skin. In addition, considering the cost and usability, future TOET light sources should be developed to be economical, simple, and easy to use to benefit patients with implanted heart rate regulator devices.

3. The development of a rechargeable coin battery with faster charging and higher power storage capacity is crucial. The rechargeable button battery used in this study has a charging capacity of 100 mAh. In contrast, the coin batteries currently used in cardiac pacemakers have a charging capacity ranging from 0.8 to 3 Ah. Therefore, there is a disparity in storage capacity between the battery used in this study and that used in current pacemakers. If the capacity of rechargeable coin batteries can approach that of primary coin batteries used in current pacemakers, the endurance of a pacemaker with a rechargeable battery would be greatly extended. It is hoped that a rechargeable coin battery with greater efficiency and storage will soon be available.

6. Conclusions

The study of remote charging for cardiac pacemakers using a TOET system has been presented. From the results of experiments performed in this study, it was found that the Zener voltage regulation circuit in the optical-energy-receiving circuit can regulate the voltage output, but it had a limited electric power output. This led to insufficient charging current and long charging time. By converting the regulation circuit to a pure resistance circuit and boosting the power of the solar cells, the output power of the circuit was significantly increased and the time required for battery charging was greatly shortened. These modifications also enabled the battery voltage to reach 2.73 V and the amperage hour to be 10 mAh. This amount of power can sustain the rhythm regulator for 20 to 35 days, depending on its mode. Therefore, transcutaneous remote charging was achieved.

References

1 Medtronic Official Site: http://www.medtronic.com
2 G. B. Bearnson, S. R. Krivoy, R. D. Jarmin, J. R. Fratto, P. Khanwilkar, K. R. Crump, and K. D. Smith: Proc. 6th Annu. IEEE Symp. Computer-Based Medical Systems (IEEE, 1993) 247–252.
3 T. Yambe, A. Tanaka, Y. Shiraishi, M. Yoshizawa, K. Abe, F. Sato, H. Matsuki, M. Esashi, Y. Haga, S. Maruyama, T. Takagi, Y. Luo, E. Okamoto, Y. Kubo, M. Osaka, S. Nanka, Y. Saijo, Y. Mibiki, T. Yamaguchi, M. Shibata, and S. Nitta: Biomed. Pharmacother. **57** (2003) 122.
4 Y. Yamagata, T. Kumagai, Y. Sai, Y. Uchida, and K. Imai: IEEE Int. Conf. Solid-State Sensors and Actuators (IEEE, 1991) 824–827.
5 Y. Yamakata, H. Matsuki, N. Chubachi, S. I. Nitta, and H. Hashimoto: IEEE Trans. Magn. **32** (1996) 5118.
6 H. Matsuki: IEEE Trans. Magn. **37** (1995) 1276.
7 Y. Mitamura, E. Okamoto, A. Hirano, and T. Mikami: IEEE Trans. Biomed. Eng. **37** (1990) 146.

8 K. Inoue, K. Shiba, K. Koshiji, K. Tsukahara, T. Ohu-mi, T. Masuzawa, E. Tatsumi, Y. Taenaka, and H. Takano: Proc. 19th Annu. Int. Conf. IEEE Engineering in Medicine and Biology Society (IEEE, 1997) 2235–2237.
9 T. Tamura, T. Togawa, A. K. M. Shamsuddin, A. Kawarada, and P. A. Oberg: Proc. SPIE Biomedical Optoelectronic Devices and Systems (1994) 99–104.
10 Philips Corporation, 50 W GU5.3 cap Warm white Halogen spot Datasheet: https://www.lighting.philips.com.tw/prof/conventionallamps-andtubes/halogenlamps/lvhalogen-withreflector/essential-lvmr16/924045517186_EU/product
11 Sinonar Corporation, SC-2723 Datasheet: https://www.alldatasheet.com/view.jsp?Searchword=2SC2723&sField=4
12 Renesas Corporation, RD3.0UH Datasheet: https://www.renesas.com/us/en/general-parts/rd30uh-diodesconstantvoltage
13 SANYO Corporation, Rechargeable Lithium Batteries Specifications, Cell Type ML2430: https://www.manualslib.com/manual/148271/Sanyo-Ml2430-Lithium.html
14 R. G. Calderhead and T. Oshita: Low Level Laser Therapy. A Practical Introduction (Wiley, New York, 1988) p. 1.
15 K. A. Ellenbogen, G. N. Kay, B. L. Wilkoff, and W. B. Saunders: Clinical Cardiac Pacing and Defibrillation (W. B. Saunders, Philadelphia, 2000) 2nd ed., p. 167.

About the Authors

Shang-Kuo Yang received his B.S. (1982) and M.S. (1985) degrees in automatic control engineering from Feng Chia University, and his Ph.D. degree (1999) in mechanical engineering from National Chiao Tung University, Taiwan. From 1985 to 1991, he was an assistant researcher and an instrumentation system engineer of the Flight Test Group, Aeronautic Research Laboratory, Zhong Shan Institute of Science and Technology, Taiwan. Since 1991, he has been with the Department of Mechanical Engineering at National Chin Yi University of Technology, Taiwan. His research interests are in reliability engineering, data acquisition system, biomedical engineering (cardiac pacemakers, patient nursing monitoring, otoliths restoration, and drunk-driving prevention), and automation.
(skyang@ncut.edu.tw)

Chia-Hong Chen received his B.S. degree in 2004 in electronics engineering from Qin Uing University of Technology and his M.S. degree in 2006 in mechanical engineering from National Chin Yi University of Technology, Taiwan. His research interests are in biomedical engineering (cardiac pacemaker) and automation. (Norman.chen67@msa.hinet.net)

Yong-Jun Zhu received his B.S. (2004) and M.S. (2009) degrees in control theory and engineering from Jiangsu University, and his Ph.D. degree (2020) in test and calibration technology and instruments from Nanjing University of Aeronautics and Astronautics, PRC. From 2004 to 2005, he was an assistant engineer of the Compal Electronic Technology (Kunshan) Co. Ltd., PRC. From 2008 to 2009, he was a senior engineer of the Hong-guang Precision Industry (Suzhou) Co., Ltd., PRC. Since 2009, he has been with the School of Electronic & Information Engineering at Suzhou University of Science and

Technology, PRC. His research interests are in image signal processing (compressed sensing), machine vision feature extraction, automotive electronics applications, weak signal detection, and automation control.
(zyj@mail.usts.edu.cn)

Kai-Jung Chen is an accomplished individual with a bachelor's degree in engineering (2010) and a master's degree in biomechanical engineering (2012) from National Cheng Kung University in Taiwan, and a Ph.D. degree in engineering from the University of Liverpool, UK (2019). From 2014 to 2019, he played a pivotal role in the Biomechanical Engineering Group at the University of Liverpool, focusing on precision ophthalmic equipment development. Since 2020, Kai-Jung has been a faculty member in the Department of Mechanical Engineering at National Chin-Yi University of Technology, Taiwan. His diverse research interests include computational biomechanics, medical assistive device development, big data and AI technology, and semiconductor and brittle material processing.
(hskchen5@ncut.edu.tw)